https://doi.org/10.5194/egusphere-2026-5259
Preprint. Discussion started: 9 September 2026

Coupling and decoupling of DIC, TA and O2 benthic fluxes along the Rhône River-dominated ocean margin.

Eva Ferreira[1], Bruno Lansard[1], Bruno Bombled[1], Christophe Rabouille[1]

[1]Laboratoire des Sciences du Climat et de l'Environnement (LSCE), CEA, CNRS, UVSQ, Université Paris-Saclay, Gif-sur-Yvette, France

Correspondence to : Eva Ferreira (eva.ferreira@lsce.ipsl.fr)

Abstract. River-dominated ocean margins (RiOMar) and their benthic compartments play a key role in coastal carbon cycling due to the combined effect of high inputs of particulate organic carbon (POC), benthic mineralization and burial processes. This study quantified benthic fluxes of DIC, TA, and oxygen along a transect influenced by riverine POC inputs, providing new insights in diagenetic processes when switching from anaerobic to aerobic dominated sediment form the river mouth to the adjacent shelf. Fluxes at the sediment-water interface were measured *ex-situ* with sediment cores incubation during two cruises at the end of spring 2018 and 2022. Stations closest to the river mouth exhibit high benthic fluxes averaging 54 ± 20, 30 ± 21 and -27 ± 14 mmol m^{-2} d^{-1} for DIC_{flux}, TA_{flux} and TOU, respectively, reflecting intense anaerobic remineralization and a strong decoupling between oxygen consumption and DIC production (DIC_{flux}:TOU ratio of 1.5 to 3.5). These large TA fluxes further support that FeS burial limits the reoxidation of reduced compounds in these sediments, allowing the upward diffusion of TA produced at depth towards bottom waters. Offshore, In contrast, shelf stations show lower flux intensities, 8 ± 3 mmol m^{-2} d^{-1} for DIC_{flux}, -1 ± 2 mmol m^{-2} d^{-1} for TA_{flux} and -9 ± 2 mmol m^{-2} d^{-1} for TOU, suggesting a greater influence of aerobic mineralization, reoxidation processes and nitrification. Stations located in the Rhône prodelta show intermediate benthic fluxes of 24 ± 11, 6 ± 4 and -17 ± 7 mmol m^{-2} d^{-1} for DIC_{flux}, TA_{flux} and TOU, respectively. By substantially expanding the spatial and temporal resolution of benthic DIC_{flux}, TA_{flux} and TOU in this system, this study provides a robust quantitative framework for assessing the contribution of RiOMar sediments to coastal alkalinity budgets and emphasizes the important role of TA fluxes released from the sediment in increasing the buffering capacity bottom waters.

1 Introduction

Within the land-sea continuum, river-dominated ocean margins (RiOMars) play a key role in the global carbon budget (Bauer et al., 2013; Regnier et al., 2022). They are important interfaces, receiving large quantities of organic and inorganic carbon from land by riverine inputs (Cai et al. 2011; Dai et al. 2012; McKee et al. 2004; Zhang et al. 2023). Dissolved nutrient inputs from rivers sustain large primary production at the ocean surface, whilst the inflow of particulate matter leads to high rates of sedimentation on the shelf, resulting in intense biogeochemical activity (Aller et al. 1996; Burdige 2007) and consequently in a net carbon flux to the atmosphere (Chou et al., 2017; Dai et al., 2022). Deltaic systems are particularly dynamic environments, with pronounced spatial and temporal variability (Gordon and Goñi 2003; Hedges et al. 1997; McKee et al. 2004). The complex interplays between organic carbon (OC) production, followed by benthic deposition, aerobic and anaerobic remineralization,

https://doi.org/10.5194/egusphere-2026-5259
Preprint. Discussion started: 9 September 2026

and preservation in coastal sediments drive the production/consumption of dissolved inorganic carbon (DIC) and total alkalinity (TA), which influences oceanic CO_2 fluxes (Emerson and Hedges 2008; Thomas et al. 2009). The partitioning between aerobic and anaerobic remineralization processes in RiOMars sediments and the associated biogeochemical fluxes across the sediment-water interface (SWI) influence bottom water properties, with potential effects on coastal acidification (Cai et al. 2011; Yin et al. 2024). Understanding the relative contributions of aerobic and anaerobic remineralization pathways and the resulting fluxes of DIC, TA, and O_2 are essential for refining carbon cycle models in RiOMar environments and along the land-sea continuum (Arndt et al. 2013; Regnier et al., 2013 and 2022).

The Rhône River prodelta, located in the Gulf of Lion (Northwestern Mediterranean Sea, France), receives substantial terrestrial inputs leading to high rates of sediment deposition, carbon burial and benthic remineralization (Lansard et al. 2009). The anoxic remineralization pathways of OC in the Rhône prodelta sediments account for nearly 85 % of the total remineralization at the river mouth and decrease off shore (Pastor et al. 2011; Ait Ballagh et al. 2021). They are largely dominated by sulfate reduction with methanogenesis close to the river mouth (Rassmann et al. 2016). These anoxic degradation processes produce significant amounts of DIC and TA, which induce biogeochemical fluxes at the SWI (Krumins et al. 2013) and potential decoupling to O_2 fluxes. Besides porewater profiles, direct measurements of benthic fluxes are required to precisely quantify the net exchange fluxes which are influenced by bioturbation, bioirrigation, sediment heterogeneity, interface processes, in order to gain a better understanding of the influence of sediments on bottom waters and the water column. In particular, the balance between TA and DIC fluxes to the bottom water determines whether these sediments act as a net source or sink of CO_2, thus influencing the buffering capacity of seawater (Andersson and Mackenzie 2012; Thomas et al. 2009). Historical measurements by Denis et al. (2003), followed by Lansard et al. (2009) and Pastor et al., (2011) were limited to oxygen and nutrient fluxes, and it is only in Rassmann et al. (2020) that DIC and TA fluxes were measured on a limited set of stations in the absence of oxygen fluxes.

For the first time, this study quantifies the benthic fluxes of DIC, TA and O_2 along an offshore transect from the Rhône River mouth to the continental shelf, which is characterized by a well-known gradient of organic carbon input (Lansard et al. 2009, Cathalot et al., 2013; Dumoulin et al., 2018; Pozzato et al., 2018). This RiOMar system serves as a case study, it allows us to examine the variability of benthic fluxes under different forcing conditions from high to low rates of OC sedimentation, anaerobic versus aerobic remineralization rates. By quantifying the benthic fluxes measured during two sampling periods, four years apart, we determine the dominant processes governing carbon cycling in these sediments. Then, we assess their implications in OC degradation and the role of aerobic and anaerobic processes in modulating benthic fluxes dynamics. Finally, a special attention is given to the total alkalinity balance, with an estimate of the contribution of each process involved in the area's alkalinity fluxes and budget.

2 Material and methods

2.1 Study area : The Rhône River prodelta

With a drainage basin of 97 800 km² and a mean water discharge of 1 700 m³ s⁻¹, the Rhône River is the main source of freshwater, nutrients and organic matter for the whole Mediterranean Sea (Ludwig et al. 2009). It delivers

https://doi.org/10.5194/egusphere-2026-5259
Preprint. Discussion started: 9 September 2026

approximately 80 % of the total riverine inputs into the Gulf of Lion, a continental shelf located in the Northwestern Mediterranean Sea (Durrieu de Madron et al. 2000; Sempéré et al. 2000). Typically, the sediment plume is driven to the south-west due to the wind forcing and the Coriolis effect (Estournel et al. 1997). Due to settling and salt-induced aggregation processes (Thill et al. 2001), approximately 60 % of the POC transported by the Rhône River accumulates in the Rhône River prodelta, a high-deposition center extending from the shoreline to approximately 70 m depth (Estournel et al. 2023; Maillet et al. 2006). Based on bathymetric profiles and sedimentation rates, the Rhône River prodelta is divided into three distinct zones (Fig.1, Got and Aloïsi 1990).

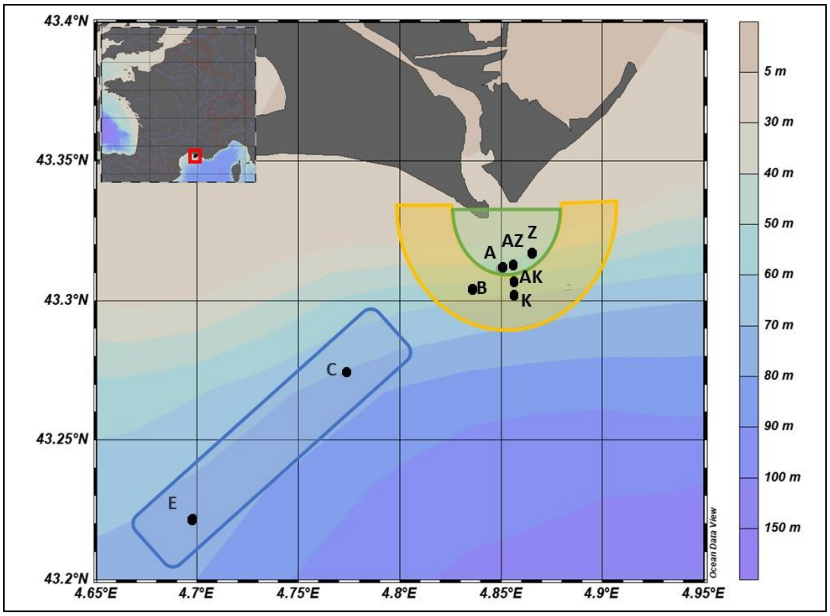

Figure 1: Map of the Rhône River mouth with the sampled stations. Identification of three zones: green semicircle for the proximal domain, yellow crescent for the prodeltaic domain and blue rectangle for the distal shelf.

The proximal domain, within 2 km of the river mouth at depths of 10-30 m, experiences the highest sediment accumulation (30-50 cm y^{-1}; Charmasson et al. 1998). The prodeltaic domain, located between 2 and 5 km offshore at depths of 30-70 m, exhibits intermediate sedimentation rates (5-10 cm y^{-1}). The distal shelf, beyond 5 km and deeper than 70 m, has the lowest sedimentation rates (< 0.1 cm y^{-1}; Miralles et al. 2005) and receives only the finest particles transported offshore.

Two oceanographic sampling cruises were carried out on board the RV *Téthys II* (FOF, Ifremer) in May 2018 (MissRhoDia 2) and 2022 (DeltaRhône 1). During each cruise, stations were sampled between 1.8 and 16.6 km from the Rhône River mouth (Fig. 1, Tab. 1), with eight stations on the first cruise (Z, A, AZ, AK, K, L, C and E) and five on the second one (Z, A, AK, K, and E). Following a southwestward transect, along the main direction of the Rhône River plume, the three main zones were sampled: the proximal domain (stations Z, A and AZ), the prodeltaic domain (stations AK, K and L) and the distal shelf (stations C and E).

https://doi.org/10.5194/egusphere-2026-5259
Preprint. Discussion started: 9 September 2026

Both cruises were carried out in late spring, a period during which the benthic system of the Rhône prodelta is sheltered from the high-discharge flood events of late fall and winter, which are the main sources of particle and organic carbon input into the system (Fig. A1).Given a relaxation time of about four months for most diagenetic processes following flood-driven perturbations (Nmor et al. 2022, Ferreira et al. 2024), and consistent with the return to reference diagenetic conditions by June–July shown by van Loenen et al. (2026, preprint), the influence of winter flood deposition on benthic fluxes is largely restrained by late spring. Sampling during this period therefore captures benthic biogeochemical fluxes reflecting the overall diagenetic pathways of organic matter degradation under quasi-stable sediment conditions.

Table 1: Sampling site, distance to the Rhône River mouth, locations and depth for all stations at each sampling periods. n.s. not sampled

		2018 (MissRhoDia 2)			2022 (DeltaRhône 1)		
Station	**Distance (km)**	**Lat. (°N)**	**Long. (°E)**	**Depth (m)**	**Lat. (°N)**	**Long. (°E)**	**Depth (m)**
Z	1.8	43°19.013	4°51.939	20	43°18.987	4°51.887	19
A	1.9	43°18.678	4°50.934	20	43°18.615	4°51.028	22
AZ	2.3	43°18.742	4°51.400	23	n.s.	n.s.	n.s.
AK	2.7	43°18.345	4°51.150	45	43°18.374	4°51.038	43
K	3.3	43°18.031	4°51.150	58	43°17.982	4°51.237	63
L	4.0	43°18.208	4°53.028	62	n.s.	n.s.	n.s.
C	8.6	43°16.283	4°46.162	71	n.s.	n.s.	n.s.
E	16.6	43°13.425	4°41.644	71	43°13.511	4°41.941	72

2.2 Bottom water sampling and analyses

Bottom water samples were collected using a 12-L Niskin bottle as close as possible to the seafloor (between 1 and 2 m above). For DIC and TA analyses, 500 mL samples were collected and stored in borosilicate bottles, poisoned with 500 µL of supersaturated $HgCl_2$, and stored in the dark at 4°C. The SNAPO-CO2 Service facilities (LOCEAN, Paris, France) conducted measurements by potentiometric titration using the closed-cell titration protocol (SOP3a, Dickson et al. 2007). Certified CO_2 seawater reference material (batch 173 and 204 provided by the Scripps Institution of Oceanography, University of California, San Diego, USA) were used to calibrate the measurements with an accuracy of ± 0.15 % (Tab. 2, Metzl et al. 2025). Temperature was measured using a thermometer with a precision of ± 0.1°C, and the salinity was measured with a conductivity based salinometer with a precision of ± 0.1. Dissolved oxygen concentrations were analyzed by Winkler titration (Hansen, 1999) immediately after sampling with a precision of ± 2 µmol L^{-1}. A 5-L bottom water tank was also filled to supply overlying water of the incubation during sampling. The water tank was kept at *in-situ* temperature close to the incubator throughout the incubation period. It was sampled and analyzed according to the same protocols as the incubation's samples for the oxygen, DIC and TA.

https://doi.org/10.5194/egusphere-2026-5259
Preprint. Discussion started: 9 September 2026

2.3 Ex situ incubations and flux measurements

Historically, a variety of methods have been used to measure benthic fluxes (Jorgensen et al. 2022; Kononets et al. 2021). The incubation of sediment cores is a well-known technique used to quantify the exchange of solutes at the SWI. The sediment cores were taken by a UWITEC® single corer (9.5 cm of internal diameter and 60 cm of length). Four sediment cores with well-preserved SWI were introduced in the incubator, where the water temperature was kept at the *in-situ* temperature and in the dark, since no benthic primary production had previously been observed in this highly turbid zone. Instrumented PVC stopper for sampling, filling directly linked to the bottom water tank and agitation were used to close hermetically the cores with O-ring (Fig. 2).

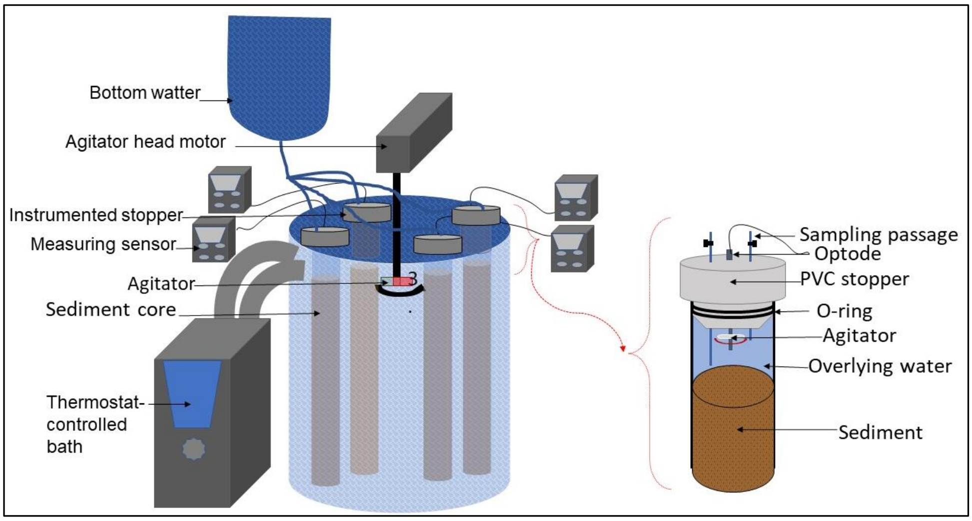

Figure 2: Schematic representation of the configuration of the ex-situ incubation experiment.

The incubated water overlying the sediment was sampled at different time intervals over a 12 or 24 hours experiment, depending on oxygen consumption rate. For TA and DIC, 10 mL of overlying water were sampled every 4h and poisoned with 10 µL of supersaturated $HgCl_2$ and stored in glass vials without headspace at 4°C until analysis. TA was measured in triplicate on 3 mL of overlying water aliquots by the open-cell potentiometric titration protocol (SOP3b, (Dickson et al. 2007), using HCl (5 mM) as titrant, resulting on a standard deviation of ± 0.2%. The HCl concentration was accurately determined in triplicate before and after each series of measurements using the same seawater reference material used for the DIC analyses. Concentrations of DIC were analyzed in triplicate of 0.75 mL samples by a LI-COR (LI-850) infrared detector, integrated in an Apollo SciTech® analyzer AS-D1, resulting on a relative uncertainty of ± 0.2%. Oxygen measurements were carried out by PyroScience's optode (Tengberg et al. 2003) at each sampling interval and by Winkler titration at the beginning and end of incubation on 12 mL samples. The results obtained for TA and DIC were corrected for the addition of bottom water from the water tank at each sampling period (27 mL). Benthic fluxes (F_i, Eq. (1)) across the SWI were calculated from the slopes (after quality controls) of the concentration-time plots and the height (H) of overlying water in each sediment core. For the calculation of total oxygen uptake rates (TOU, in mmol m^{-2} d^{-1}), the slope of oxygen concertation versus time was determined on the first 25-30% decrease from the initial oxygen concentration within the incubation, following the recommendations given by (Kononets et al. 2021)

https://doi.org/10.5194/egusphere-2026-5259
Preprint. Discussion started: 9 September 2026

$$F_i = H * \frac{dCi}{dt} \quad (1)$$

2.4 Statistical tests

Non-parametric Mann Whitney tests were performed on all the data set and on each domain, to assess the interannual comparison of benthic fluxes between the two sampling campaigns (2018 and 2022). The tests were conducted on DIC and TA benthic fluxes as the mean variables of benthic biogeochemical processes which provides a robust indicator of sediment–water exchange variability. They were performed only on the stations that were sampled during both campaigns, ensuring a strict station-to-station comparison and avoiding spatial bias.

2.5 Calculation of alkalinity mass balance

As summarized in Table 2 (see also Hu and Cai, 2011), a limited number of processes can lead to a net production of total alkalinity leading to fluxes to the water column: aerobic mineralization associated to nitrification, denitrification, $CaCO_3$ dissolution and precipitation, and FeS (or Pyrite) burial.

Table 2 : Reactions leading to TA production or consumption in marine sediments. All values for TA and O_2 normalized to 1 DIC production. Note that FeS precipitation can arise following different pathways (biotic or abiotic, Rassmann et al., 2020) and lead to variable ratio of TA production to FeS burial. Here, we adopted an average value of 3*

	Reaction	ΔTA	ΔDIC	ΔO_2
Aerobic mineralization + nitrification	$(CH_2O)_{106}(NH_3)_{16} + 138\ O_2 \rightarrow 106\ HCO_3^- + 16\ NO_3^- + 122\ H^+ + 16\ H_2O$	- 0.15	+ 1	-1.3
Denitrification	$(CH_2O)_{106}(NH_3)_{16} + 84.8\ NO_3^- \rightarrow 106\ HCO_3^- + 16\ NH_4^+ + 42.4\ N_2 + 5.2\ H^+ + 42.4\ H_2O$	+ 0.8	+ 1	/
Carbonate dissolution	$CaCO_3 + 16\ H_2O + CO_2 \rightarrow 2\ HCO_3^- + Ca^{2+}$	+ 2	+ 1	/
Carbonate precipitation	$2\ HCO_3^- + Ca^{2+} \rightarrow CaCO_3 + 16\ H_2O + CO_2$	-2	-1	/
FeS precipitation and burial*	$(CH_2O)_{106}(NH_3)_{16} + 47.1\ SO_4^{2-} + 47.1\ Fe(OH)_3(s) \rightarrow 106\ HCO_3^- + 16\ NH_3 + 47.1\ FeS(s) + 11.7\ H^+ + 117\ H_2O$	+ 1.15 TA/FeS + 2.6*	+ 1	/
	$(CH_2O)_{106}(NH_3)_{16} + 53\ SO_4^{2-} + 35.3\ Fe(OH)_3(s) \rightarrow 106\ HCO_3^- + 16\ NH_3 + 17.7\ S_0 + 35.3\ FeS(s) + 106\ H_2O$	+ 1.15 TA/FeS + 3.4*		

The aerobic mineralization rates and denitrification were taken from modelling studies of Pastor et al. (2011) and Ait Ballagh et al. (2021). Calcium carbonate dissolution rates were adopted from Ferreira's thesis (2025) showing the absence of dissolution in all zones of the prodelta and adjacent shelf, and $CaCO_3$ precipitation was taken from Rassmann et al. (2016) for the proximal zone only who assumed 10-15% of anaerobic mineralization leading to carbonate precipitation. According to Pastor et al. (2011) aerobic mineralization represents 10% of total mineralization, which were subtracted from the DIC flux to get to the anaerobic mineralization rate. FeS burial was estimated using Rassmann et al. (2020) in which they report values for the proximal, prodelta and distal zones). Unlike Rassmann et al. (2020), who adopted a conservative estimate of 2 for the TA flux to FeS burial, we chose to average the two pathways (biotic and abiotic, Tab. 2) and ended up with a ratio of 3.

3 Results

3.1 Bottom water characteristics

Bottom water properties were very similar for both cruises at the same station four years apart (Tab. 3). For all stations, bottom water salinity ranged from 37.2 in 2022 at station AZ, located close to the river mouth, to 38.3 in 2018 at station K, located on the shelf. Bottom water temperature ranged from 14.7 °C, at station C in 2018, to 20.6 °C, at station AZ in 2022, decreasing along the transect with depth. The bottom waters of the two stations Z and A, situated in front of the Rhône River mouth and therefore shallower, were warmer in 2022 than in 2018, with a mean difference of +2°C between the two sampling periods. This trend is not reflected in the stations further offshore. TA concentrations remained similar between 2018 and 2022 across all stations, averaging 2565 ± 6.1 µmol kg^{-1}. Bottom waters were well ventilated, with oxygen concentrations ranging from 277 µmol L^{-1}, at station A in 2018, to 219 µmol L^{-1}, at station E, in 2022, also decreasing along the transect with depth. We observed an increase in DIC concentration of 25 ± 5 µmol kg^{-1} between 2018 and 2022 but only at the deepest stations. This increase in DIC in the bottom waters offshore is likely due to OC mineralization and exchanges with the sediments.

3.2 Benthic flux distribution

The benthic fluxes of DIC, TA and O_2 were studied as a function of the distance from the Rhône River mouth, with average fluxes by area decreasing along the transect for all three parameters (Fig. 3, Fig. B1, Fig. C1.). For DIC_{flux}, the highest fluxes were observed in the proximal domain, with an average of 54 ± 20 mmol m^{-2} d^{-1}. This shallow zone demonstrated spatial and temporal variability, with high standard deviations observed between fluxes. Deeper, in the prodeltaic domain, benthic DIC fluxes declined by 56% compared to the proximal domain with an average of 24 ± 11 mmol m^{-2} d^{-1}. The heterogeneity remained at a high level in the prodeltaic domain, both within and between stations. In the distal shelf, all benthic fluxes were 86 % lower than those observed in the proximal domain, with an average of 8 ± 3 mmol m^{-2} d^{-1} and a greater homogeneity. With regards to TA fluxes the proximal domain showed most intense fluxes, with an average of 30 ± 21 mmol m^{-2} d^{-1}, also presenting strong intra-zone variations. In the prodelta, a rapid drop of TA fluxes was observed, representing one-fifth of the flux previously recorded in the proximal domain, average of 6 ± 4 mmol m^{-2} d^{-1}, again with a strong heterogeneity. The distal shelf was characterized by extremely low or even negative TA fluxes, with an average of -1 ± 2 mmol m^{-2} d^{-1}. The TOU followed a similar trend as the previous two parameters, with less contrast along the transect. In the proximal domain, TOU rates averaged 27 ± 14 mmol m^{-2} d^{-1}, while in the prodeltaic domain they fell by 40%, and by almost 65%, to 9 ± 2 mmol m^{-2} d^{-1} in the distal shelf.

https://doi.org/10.5194/egusphere-2026-5259
Preprint. Discussion started: 9 September 2026

Table 3: Physicochemical parameters of bottom water for all stations at each sampling period. n.s. not sampled.

Station	2018 (MissRhoDia 2)						2022 (DeltaRhône)					
	Date (dd/mm)	Salinity	Temp. (°C)	DIC (µmol kg^{-1})	TA (µmol kg^{-1})	Oxygen (µM)	Date (dd/mm)	Salinity	Temp. (°C)	DIC (µmol kg^{-1})	TA (µmol kg^{-1})	Oxygen (µM)
Z	22/05	38.0	15.7	2278	2568	273	23/05	37.9	18.7	2275	2564	257
A	23/05	37.8	15.6	2271	2559	277	20/05	38.1	18.6	2273	2553	255
AZ	01/06	38.1	19.5	2266	2567	243	n.s.	n.s.	n.s.	n.s.	n.s.	n.s.
AK	26/05	37.9	15.6	2270	2561	264	22/05	38.0	15.9	2297	2567	252
K	29/05	38.3	15.7	2272	2561	261	19/05	38.0	15.3	2291	2564	251
L	31/05	38.1	15.1	2304	2575	235	n.s.	n.s.	n.s.	n.s.	n.s.	n.s.
C	24/05	38.2	14.7	2309	2568	227	n.s.	n.s.	n.s.	n.s.	n.s.	n.s.
E	25/05	38.3	14.8	2298	2566	235	21/05	38.1	14.5	2327	2563	220

https://doi.org/10.5194/egusphere-2026-5259
Preprint. Discussion started: 9 September 2026

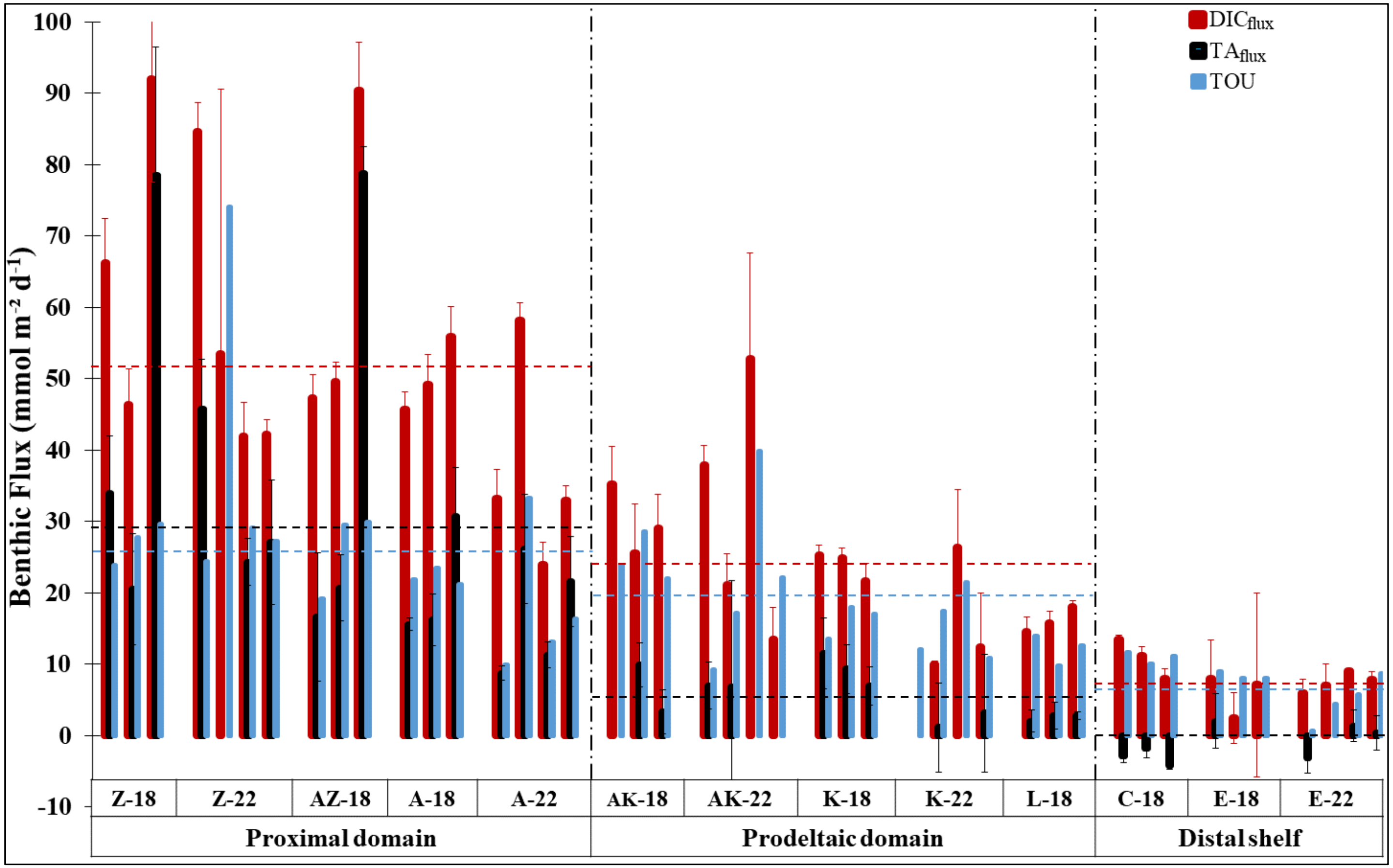

Figure 3: Benthic DIC_{flux} (red), TA_{flux} (black) and TOU (blue, in absolute values) along the investigated transect from the Rhône River mouth to the Shelf. A positive value indicates that the flux is directed from the sediments towards the bottom waters. Dotted lines correspond to the mean values for each parameter's fluxes by area.

https://doi.org/10.5194/egusphere-2026-5259
Preprint. Discussion started: 9 September 2026

3.3 Statistical analysis

Results provide by the Mann Whitney tests indicate no statistically significant difference (p value > 0.05) between the two sampling periods for benthic fluxes for any of the domain considered (proximal, prodeltaic and distal shelf; Tab. 4). The proximal section shows a p-value close to the conventional significance threshold (p value = 0.06), with generally higher water discharge observed in 2018, this difference does not reach the threshold for statistical significance. This trend may reflect differences in environmental conditions between the two sampling periods, notably variations in water discharge and the associated deposition and burial of organic matter, which do not, however, result in significantly different fluxes in this highly dynamic area. This statistical consistency supports the integration of the two periods (2018 and 2022 datasets) into a single combined dataset for each domain.

Table 4 : Parameter of Mann Whitney statistical tests performed on DIC and TA benthic fluxes for each domain between 2018 and 2022 data.

	Mann Whitney p value DIC_{flux}	Mann Whitney p value TA_{flux}
All data	0.23	0.42
Proximal	0.06	0.32
Prodeltaic	0.13	0.25
Distal shelf	0.24	0.36

We further used statistical tests to compare the zones: although there is some continuity between the proximal and prodelta zones (A and AK in 2022), the statistical tests carried out on each couple of zones clearly highlight a significant difference between the three zones for all parameters (Tab. 5; p < 0.05), supporting the distinct study of the three zones.

Table 5 : *Parameter of Mann Whitney statistical tests performed on DIC and TA benthic fluxes for each couple of domains.*

	Mann Whitney, p value DIC_{flux}	Mann Whitney, p value TA_{flux}
Proximal vs. Prodeltaic	$1.7 * 10^{-5}$	$9.7 * 10^{-6}$
Prodeltaic vs. Distal shelf	$3.1 * 10^{-5}$	$3.6 * 10^{-4}$
Proximal vs. Distal shelf	$9.9 * 10^{-6}$	$3.5 * 10^{-5}$

https://doi.org/10.5194/egusphere-2026-5259
Preprint. Discussion started: 9 September 2026

3.4 DIC flux versus TOU

According to **Figure 4, Appendix 2** and **3**, there are marked differences between the three zones. The DIC_{flux} and TOU are generally low in the distal area on the shelf and DIC_{flux}:TOU ratios are characterized by a distribution around 1:1, with a homogeneous group of data. On the other hand, with larger DIC_{flux} and TOU levelling off below 30 mmol m^{-2} d^{-1}, the DIC_{flux}:TOU ratios in the proximal domain diverge from the 1:1 ratio, with values of up to 3.5. Data from the prodeltaic domain show a dynamic transition between the two groups, with one part of the data aligned with ratios of 1 when DIC fluxes are low, while the other is gradually shifting away from this trend, with a strong heterogeneity.

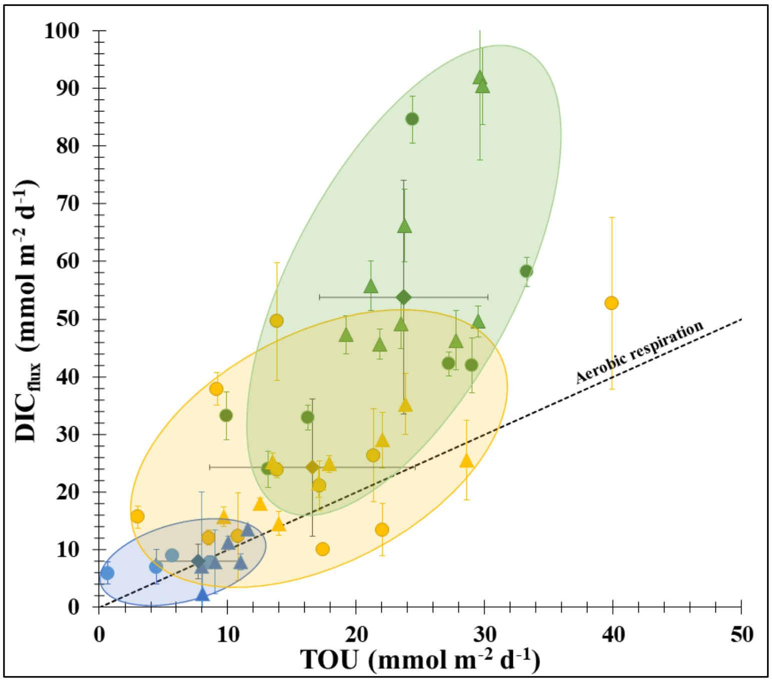

Figure 4 : Benthic DIC_{flux} as a function of TOU rates. The triangles represent the 2018 data and the circles the 2022 data. The green area corresponds to the proximal domain, the yellow one envelops the prodeltaic domain and the blue one indicated the distal shelf. The dark diamonds in the respective colors represent the average of all stations in each zone for all campaigns combined. Dotted line represents the characteristic slope of 1.

3.5 TA versus DIC fluxes

TA and DIC fluxes show a large variation along the transect. with significant differences observed in the three investigated zones (Fig. 5). All TA_{flux}:DIC_{flux} ratios measured in this study are below 1. In the proximal area, TA and DIC fluxes are large and TA_{flux}:DIC_{flux} ratios are clearly higher than in the other two areas. The TA_{flux}:DIC_{flux} show an average ratio of 0.52, with a marked dispersion in flux magnitude between stations, regardless of the year. In contrast, in the distal area and part of the prodelta, the fluxes are much lower especially for TA with some negative values and TA_{flux}:DIC_{flux} ratios cluster around 0 with less variability, forming a more compact group. Between these two extremes, the prodeltaic area displays an intermediate behavior, with stations displaying very

https://doi.org/10.5194/egusphere-2026-5259
Preprint. Discussion started: 9 September 2026

low fluxes and others with significant fluxes, reflecting a spatial gradient between the proximal and the distal area.

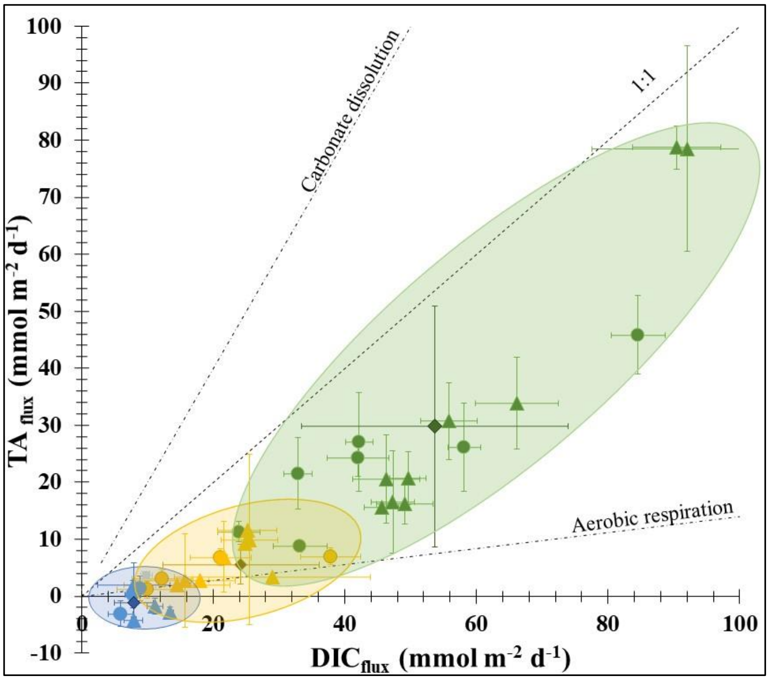

Figure 5 : Benthic TA_{flux} as a function of DIC_{flux}. Triangles represent the 2018 data and circles 2022 data. Green area corresponds to the proximal domain, yellow envelops the prodeltaic domain and blue indicates the distal shelf. The diamonds in the respective colors represent the average of all stations in each zone for all campaigns combined. The different dotted lines correspond to the respective characteristic ratios of carbonate dissolution (2:1) and aerobic respiration (0.15). See Table 2 for further details on the reaction equations.

4 Discussion

4.1 Benthic flux distributions along the Rhône River mouth-to-shelf gradient

Due to the inflows from the Rhône River, the organic carbon content in surface sediment ranges from more than 1.8%, in the proximal domain, to less than 0.8%, in the shelf (Lansard et al., 2009). This RiOMar system offers the opportunity to study DIC, TA and TOU benthic fluxes, and their coupling, under contrasting biogeochemical regimes, ranging from anaerobic to aerobic dominated conditions within the sediments. A clear spatial gradient from the Rhône River mouth to offshore emerges from the dataset (Fig. 3).The highest benthic fluxes were observed in the proximal and prodeltaic domains, which act as significant sources of DIC and TA to the bottom waters. In the proximal domain, DIC fluxes range from 30 to 90 mmol m^{-2} d^{-1}, in good agreement with previous benthic fluxes quantified in the same zone (18-78 mmol m^{-2} d^{-1}, Rassmann et al. 2020). These results can also be compared with previous data obtained in other RiOMar systems such as the northern Gulf of Mexico with the Mississippi River. Benthic DIC fluxes were there quantified by *in-situ* benthic chamber with values ranging from 15 to 75 mmol m^{-2} d^{-1} (Magette et al. submitted) and from 36 to 53 mmol m^{-2} d^{-1} (Rowe et al. 2002). In our study, TA fluxes measured in the proximal zone reached up to 80 mmol m^{-2} d^{-1}, a relatively high value for this parameter

https://doi.org/10.5194/egusphere-2026-5259
Preprint. Discussion started: 9 September 2026

(14-75 mmol m^{-2} d^{-1}, Rassmann et al. 2020). In comparison, these values are slightly higher, though of the same order of magnitude, as values reported in other deltas such as the Danube and the Dniester (21-67 mmol m^{-2} d^{-1}; Friedl et al. 1998) and the Mississippi (40-50 mmol m^{-2} d^{-1}, Magette et al. submitted).

The intensity of all benthic fluxes decreases rapidly with depth and distance from the river mouth. This sharp decline is consistent with previous observations of an exponential decrease in sediment accumulation rates and TOU with distance from the Rhône River mouth (Cathalot et al. 2010; Lansard et al. 2009; Pastor et al., 2011). A similar sharp decrease is observed in our dataset, particularly for DIC, with a much larger amplitude: a drop by a factor of 7 is observed between the average values from the proximal domain to the distal shelf (Fig. 3) compared to a drop by a factor of 3 for average TOU. Ait Ballagh et al. (2021) similarly reported a reduction by a factor of 16 in modeled OC remineralization fluxes between station Z and station E, as distance from the river mouth increased and organic matter inputs declined. Although the magnitude of this decrease is larger in the model outputs, it follows the same decreasing trend as the observed DIC fluxes. The organic matter composition and reactivity, as characterized in 2018 (Dumoulin et al., 2026), is consistent with previous work in the Rhône prodelta which showed that (i) sedimentary OM becomes progressively less reactive with increasing distance from the river mouth, based on POC, PON, $\delta^{13}C$ and $\Delta^{14}C$ analyses (Cathalot et al., 2013; Dumoulin et al., 2018; Pozzato et al., 2018) and (ii) the most labile fraction of POC is delivered by the river in the proximal and prodelta zones, while marine production provides a more limited and less reactive input on the shelf. Therefore, the observed decrease in benthic fluxes is likely related to a transition from intense aerobic and anaerobic mineralization fueled by relatively labile organic matter near the river mouth to lower mineralization rates offshore where more refractory POC predominates and marine inputs are limited (Lansard et al., 2009; Pastor et al., 2011; Rassmann et al., 2016). At the most distal stations, low and occasionally negative TA fluxes (between -2 and -4 mmol m^{-2} d^{-1}) were observed (Station C-18, E-22). Although these fluxes are small, and derived from limited concentration changes during the incubation experiments, they exceeded the measurement uncertainty and thus remained significant and negative. Processes linked to the nitrogen cycle can explain these low and negative fluxes and will be discussed in section 4.3.

The observed benthic fluxes also show marked spatial heterogeneity at all scales which can be explained by several factors. First the distance between the stations within a same group, which can extend to several kilometers (Fig. 1), may induce different depositional patterns near the river mouth in the proximal and prodeltaic domains. Indeed, these two zones are characterized by massive and rapid deposition in winter, known as active and powerful biogeochemical reactors (Aller et al. 1996; Rassmann et al. 2016). These deposition modes may produce heterogeneous deposition in quantity and quality of organic matter generating internal variability in remineralization fluxes within each zone and thus give rise to intra-group variability. Second small scale (centimeter to meter) heterogeneity may be linked to bioturbation, local preferential deposition of fresh organic matter in holes and trenches (Glud et al. 2009). Large heterogeneities are indeed observed at the intra-station scale based on fluxes from several cores. This heterogeneity has also been evidenced in various porewater profiles carried out in the same areas (Ait Ballagh et al. 2021; Rassmann et al. 2020).

The decrease in the benthic fluxes follows distinct patterns along the offshore transect, resulting in shifts in TA_{flux}:DIC_{flux} ratios and DIC_{flux}:TOU ratio (Fig. 6). These shifts reflect diversity of underlying biogeochemical processes that generate these fluxes. To guide the interpretation of the observed fluxes, it is important to get insight into the aerobic/anaerobic diagenetic processes involved based on numerous existing literatures, and to examine their net influence on DIC, TA and O_2 fluxes and their ratios at each site.

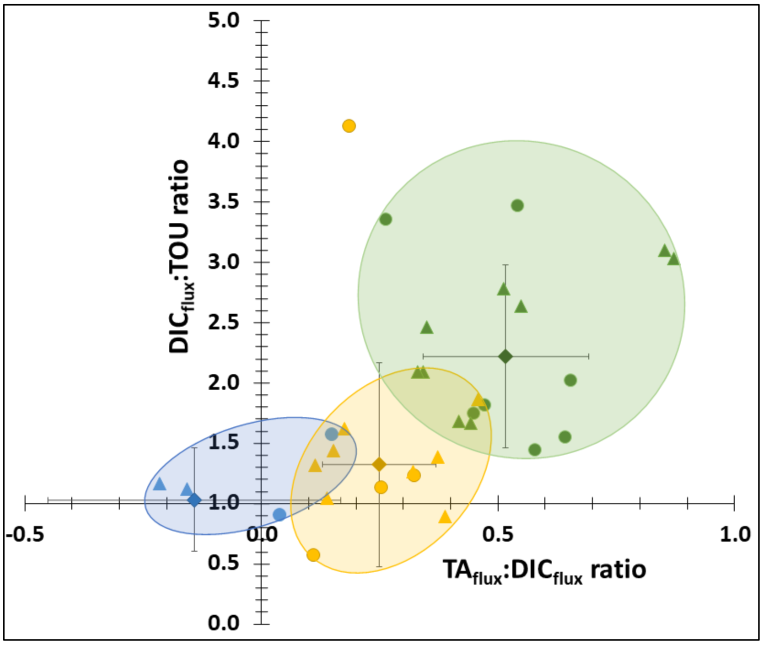

Figure 6: DIC_{flux}:TOU ratio as a function of TA_{flux}:DIC_{flux} ratio. The triangles represent 2018 data, the circles 2022 data. Green correspond to proximal domain, yellow to the prodeltaic domain and blue to the distal shelf. The diamonds in the respective colors represent the average of all stations in each zone for all campaigns combined.

4.2 Spatial evolution of TOU and DIC benthic fluxes along the transect

The spatial variations of TOU and DIC benthic fluxes are the consequence of large changes in diagenetic processes from the river mouth to the adjacent shelf as evidenced in earlier papers (Pastor et al., 2011, Cathalot et al., 2013, Rassmann et al. 2021). In the distal shelf and the prodeltaic domain, where DIC fluxes are roughly below 10 mmol m^{-2} d^{-1}, indicating a limited organic carbon recycling intensity, a 1:1 relationship between TOU and DIC fluxes is mostly observed. This relationship suggests that remineralization is well-coupled to oxygen consumption in these two areas, with limited contribution of anaerobic processes on the recycling of organic carbon. Here, most of the OC remineralization is accomplished by aerobic respiration (Pastor et al. 2011) which consumes O_2 and produces CO_2 at equivalent molar rates, without significant TA production. The limited anaerobic remineralization (mostly Fe and Mn oxide reduction, see Pastor et al., 2011) gives rise to reduced dissolved metals (Mn^{2+} and Fe^{2+}) which are completely re-oxidized by oxygen in the thick oxic layer (Rassmann et al., 2020), therefore preventing reduced compounds to escape from the system. The stoichiometry of the system is thus similar to the aerobic remineralization.

In contrast, the proximal domain, that receives the largest input of OC from the Rhône River, shows a significant

https://doi.org/10.5194/egusphere-2026-5259
Preprint. Discussion started: 9 September 2026

departure to the closed system relationship of 1:1. Fluxes of DIC are marked by a significant increase in this area with values ranging between 30 mmol m^{-2} d^{-1} and 90 mmol m^{-2} d^{-1}. Very high DIC concentrations (> 40 000 µmol kg^{-1}) were reported in the porewater of these sediments (Ait Ballagh et al. 2021; Rassmann et al. 2020), reflecting intense remineralization of OM. This large increase of DIC fluxes is decoupled from the TOU whose evolution which levels off, therefore generating a steep DIC_{flux}:TOU ratio slope up to 3.5 at station Z (Fig. 6). Such high ratios indicate a dominant contribution of anaerobic respiration to OC remineralization and a burial of reduced compounds (Hu and Cai, 2011), where substantial DIC is produced without proportional oxygen consumption (Pastor et al. 2011).

The decoupling between O_2 consumption and OC remineralization, as quantified by the DIC flux, can only occurs if (i) a loss of reduced elements (Fe^{2+}, Mn^{2+}, H_2S) occurs to the overlying water by outfluxing or to deeper sediments by burial (Rassmann et al. 2020), or (ii) because of an intense dissolution of calcium carbonate releasing substantial DIC to the porewater. Rassmann et al. (2016 and 2020) showed that dissolution of carbonate is limited and that $CaCO_3$ precipitation dominates in the deep sediment layers of the proximal domain. Reduced element flux to the water column is unlikely (Fe^{2+} appears at several cm depth, and bio-irrigation is limited), therefore leaving burial of combined reduced elements as the only possible explanation for the DIC to O_2 flux decoupling in the proximal domain, as shown in Rassmann et al. (2020).

Denitrification is another candidate for a DIC-O_2 decoupling. However, given the low nitrate concentration in bottom waters of the proximal zone, denitrification is minimal in these sediments, representing at most a few percent of aerobic respiration (Pastor et al., 2011; Ait Ballagh et al., 2021) which induces a shift towards processes such as dissimilatory iron and manganese reduction and sulfate reduction.

Sulfate reduction is the dominant remineralization process in the Rhône prodeltaic domain (Ait Ballagh et al. 2021), as it is the case in most organic-rich coastal sediments (Burdige and Komada 2011; Canfield et al. 1993) but Fe-oxide reduction is significant (Rassmann et al. 2020). These anaerobic reactions release both DIC and TA as well as reduced species (Fe^{2+} and H_2S), which can precipitate insoluble FeS and be permanently buried and preserved. Therefore, it limits their reoxidation in the upper layers (Aller et al. 1986; Rassmann et al. 2020) especially in sediments with high sedimentation rates and creates a strong decoupling between O_2 and DIC fluxes. It is noteworthy that the burial of reduced compounds at depth within the sediment, as proposed here to explain the decoupling between TOU and DIC fluxes in the proximal zone, should also be linked to a positive efflux of TA (Hu and Cai, 2011; Rassmann et al. 2020). Indeed, in case of significant burial of reduced elements, TA consumption in surface sediments due to re-oxidation is substantially lower than TA production inside the sediments by anoxic diagenetic pathways. This disequilibrium between TA sources and sinks can generate large TA fluxes at the sediment-water interface (Hu and Cai, 2011).

4.3 Variations of TA fluxes along the offshore transect

TA_{flux}:DIC_{flux} ratios were always below 1 at all stations (Fig. 6) which means that net DIC production is larger than net TA production. These large values calculated for the proximal zone and the rapid decrease of this ratio offshore suggests that anaerobic respiration significantly contributes to remineralization near the Rhône River mouth and that aerobic respiration dominates in the low DIC flux regions. A distinction between the three domains

https://doi.org/10.5194/egusphere-2026-5259
Preprint. Discussion started: 9 September 2026

is obvious (Fig. 5), allowing us to deepen our understanding of TA-producing processes in sediments. Spatial differentiation of the diagenesis dynamics and redox conditions illustrates how local system characteristics control benthic biogeochemical fluxes along the transect.

In the distal shelf and in the distal part of the prodelta, TA fluxes appear to be extremely low (between 0 and 5 mmol m^{-2} d^{-1} or even negative), and are associated with relatively low DIC fluxes, under 20 mmol m^{-2} d^{-1}. These results are in good agreement with theoretical and experimental estimates (Anderson et al. 1986; Wolf-Gladrow et al. 2007). In these shelf sediments, the low TA fluxes are further explained by the closed redox cycle in which burial of reduced inorganic compounds such as FeS or pyrite is limited by very low sulfate reduction and low sedimentation rates. As a consequence, a complete reoxidation of reduced compounds (Fe^{2+}, Mn^{2+}) occurs in the upper sediments. In the process, O_2 is consumed stoichiometrically, and TA decreases during re-oxidation by the large production of H^+ generated at the anoxic-oxic interface (Hu and Cai, 2011). By restoring the balance between alkalinity production, by anaerobic remineralization of OM, and consumption of reduced species, by reoxidation, these processes limit the net production of TA and the TA_{flux} is consequently very low.

The negative TA fluxes occasionally observed at distal stations can be attributed to an imbalance between denitrification and nitrification processes (Van Dam et al. 2022). Denitrification is involved in OM degradation, producing TA, while nitrification leads to the consumption of TA. A nitrification rate higher than that of denitrification may thus lead to negative fluxes of TA, as observed in the German Bight (Van Dam et al. 2022). In our case, this hypothesis is supported by the presence of significant NH_4^+ concentrations at depth in porewaters at the distal stations (>100 µM; Denis and Grenz, 2003; Pastor et al. 2011), that are completely consumed in surface sediments (Ait Ballagh et al. 2021) leading to outward fluxes of NO_3^- (0.2 - 0.3 mmol m^{-2} d^{-1}) and very low fluxes of NH_4^+ were observed at an equivalent station (station G) in March and June (Denis and Grenz 2003). The TA mass balance (Fig. 7) based on previous literature estimates of process rates also indicates a slight imbalance towards nitrification for the distal zone and suggest negative TA benthic fluxes in this zone (i.e. TA entering the sediment).

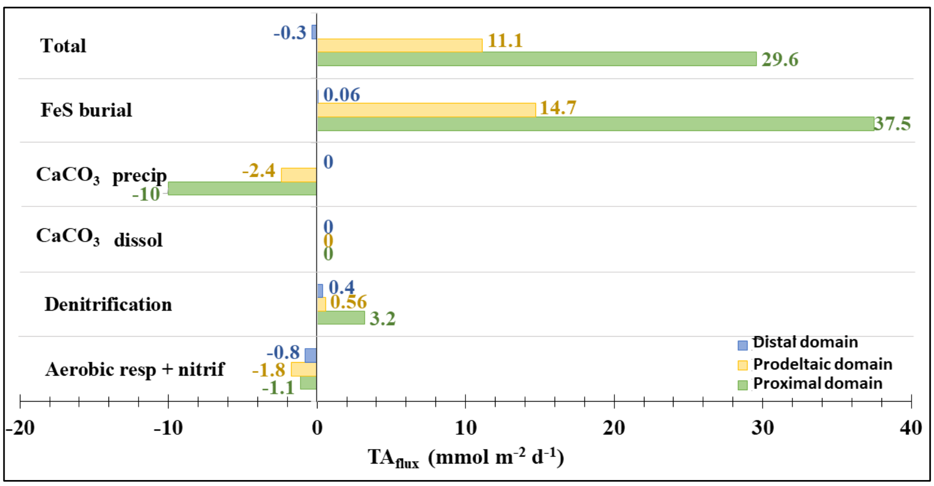

Figure 7: Processes generating/consuming TA in sediments studied and the mass balance of these processes (Total)

https://doi.org/10.5194/egusphere-2026-5259
Preprint. Discussion started: 9 September 2026

leading to potential net fluxes from the sediments of the Rhône prodelta and the Gulf of Lion to the bottom waters, according to the literature (Ait Ballagh 2021; Pastor et al., 2011; Rassmann et al., 2020; Ferreira, 2025; Rassmann et al., 2016).

As diagenetic activity intensifies in the proximal domain and some stations of the prodelta, TA_{flux} rise significantly, reaching values as high as 79 mmol m^{-2} d^{-1} (average of 30 ± 21 mmol m^{-2} d^{-1}) and TA_{flux}:DIC_{flux} ratios averaging 0.55 (range 0.3-0.9). These elevated ratios and TA_{flux} are strongly correlated with the decoupling of DIC_{flux} and TOU (Fig. 6), suggesting a link between the redox cycle and TA net flux. The alkalinity balance (Fig. 8) indicates that, in the proximal zone, FeS burial is the largest process generating TA. The link between enhanced TA fluxes and the increased burial of reduced sulfur-iron solid phases is rather indirect. As burial of reduced solid phases (especially FeS) increases in proximal sediments with high sedimentation rates, the reoxidation of reduced species at the oxic interface and therefore alkalinity consumption near the sediment-water surface is lowered (Hu and Cai, 2011; Lukawska et al. 2018; Rassmann et al. 2020). This limited reoxidation allows a significant fraction of the TA produced during anaerobic remineralization to diffuse out, resulting in significant alkalinity fluxes across the SWI. The burial of reduced element, such as FeS, is typically observed in systems subject to high POC inputs and large sedimentation rates such as subaqueous deltas. Similar dynamics have been reported in the Gulf of Gdańsk (Baltic Sea), where intensive sulfate reduction and anaerobic oxidation of methane are major internal sources of TA (Lukawska-Matuszewska and Dwornik 2025). In the earlier study dealing with TA fluxes by Rassmann et al. (2020), a very limited number of fluxes was measured in the proximal and distal stations. Thus, it did not fully capture the gradual change and the thresholds of biogeochemical fluxes in the area, especially the transition zone of the prodeltaic domain which was not sampled. This paper addresses this limitation by incorporating multiple stations across the transect over two different sampling years with replicate measurements, thereby providing a more robust, spatially comprehensive, study.

Because FeS burial links TA fluxes with the redox cycle and especially re-oxidation, it is expected that increase in TA_{flux}:DIC_{flux} ratio be accompanied by a rise in DIC_{flux}:TOU ratio, clearly visible on Figure 6. Conversely, in lower DIC flux regions, DIC_{flux}:TOU ratio is close to 1, indicative of oxic recycling and full reoxidation of reduced species, i.e. the closed system seen in the distal shelf and part of the prodelta. In this case, TA:DIC flux ratios remain close to zero. The threshold between these two regimes is around 20 mmol m^{-2} d^{-1} for DIC flux, with most shelf sediments falling below this threshold (Krumins et al., 2013; Van de Velde et al., 2025). The large dispersion of values, particularly within the proximal zone (green circle in Fig. 6) suggest that heterogeneity is large in this high sedimentation area subject to rapid flood deposits. In addition, other unquantified processes such as pyrite production and burial or Anaerobic Oxidation if Methane (AOM) due to shallow SO_4 depletion and methanogenesis could affect unevenly the TA balance, but their magnitudes are presently not known.

The other class of processes that largely affect TA fluxes is linked to calcium carbonate (dissolution and precipitation, van de Velde et al., 2025). As emphasized by Ferreira (2025), carbonate dissolution is undetectable in the Rhône prodelta and shelf sediments, hence this flux is set to zero in the alkalinity balance (Fig. 7). On the opposite, carbonate precipitation is present in proximal and prodelta domains and represents 10-15% of anaerobic DIC production within the sediments (Rassmann et al., 2016). The precipitation of $CaCO_3$ represents a substantial TA sink in proximal sediments (25-30% of FeS burial) and a limited sink in prodelta sediments (10%).

Overall the alkalinity balance suggests a pattern with a large decrease of TA fluxes from the proximal to the distal zone with the prodelta being intermediate (Fig. 7). Using this independent mass balance from the literature, the calculated TA fluxes match well with the measured TA fluxes from this study, with a shift between extremely high values in the proximal zone to slightly negative values in the distal shelf (Tab. 6).

Table 6: Benthic fluxes of TA calculated by mass balance based on processes from the literature (see section 2.5 for details) and average TA fluxes measured in this study.

TA benthic flux (mmol m^{-2} d^{-1})	Proximal	Prodelta	Distal
Mass balance calculated	30	11	-0.3
Measured average	30 ± 21	6±4	-1 ± 2

5 Conclusion

This work contributes to reduce the uncertainties in DIC and TA benthic fluxes and TOU estimates, providing critical insights into the role of RiOMar sediments in the global carbon cycle. We have evidenced a strong biogeochemical gradient in benthic fluxes along the offshore transect, influenced by organic inputs from the Rhône River. Large benthic fluxes of DIC and TA were measured at proximal stations near the river mouth, associated with intense mineralization of organic matter dominated by anaerobic processes, and a marked decoupling between oxygen consumption and total mineralization. Further offshore in distal stations, TA fluxes are low or even negative, suggesting an important oxic mineralization, large re-oxidation rate of reduced compounds and a dominance of nitrifying processes. These findings also provide further support for the hypothesis that burial of combined reduced metabolites (e.g. FeS) limits the reoxidation processes and allows the TA produced deeper to be transported to the bottom water (Rassmann et al. 2020).

Although the fluxes collected in the late spring over two different years did not statistically vary, the temporal dynamics of these fluxes should not be forgotten. Indeed, the Rhône prodelta system is subject to strong seasonal variations, with large floods in winter and intense droughts / heat waves in summer. By modifying the input of organic matter, nutrients and particles, these hydrological events could influence the biogeochemical structure of sediments and associated benthic fluxes (Ferreira et al. 2024; Nmor et al. 2022), thus potentially modifying the annual budget. This expanded dataset allows for a more robust characterization of benthic fluxes of DIC, TA, and O_2 along one land-sea continuum in the late spring period. However, it will need to be supplemented by annual time-series studies, as is the case in most RiOMars systems around the world, in order to reduce uncertainties relating to the carbon cycle along the land-sea continuum.

https://doi.org/10.5194/egusphere-2026-5259
Preprint. Discussion started: 9 September 2026

Appendix A

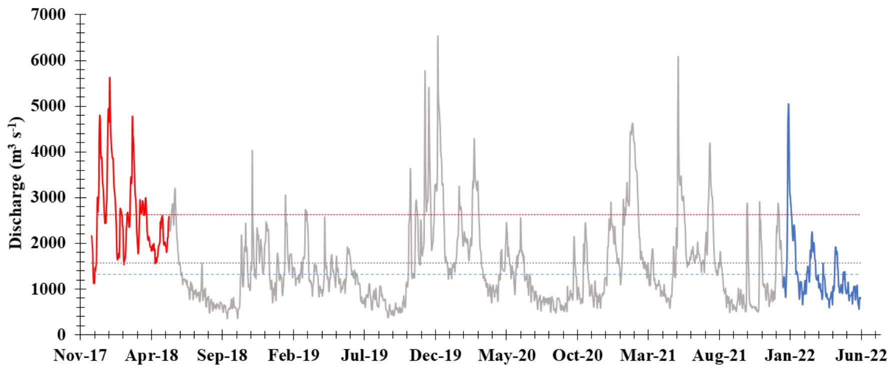

Figure A1 : *Mean daily water discharge of the Rhône River at Beaucaire-Tarascon. Red corresponds to December 2017-June 2018 period, blue corresponds to December 2021-June 2022 period. Grey corresponds to the periods in between the 2 cruises. Dotted lines symbolize the average water discharge level of each period.*

https://doi.org/10.5194/egusphere-2026-5259
Preprint. Discussion started: 9 September 2026

Appendix B

		MissRhoDia2 - 2018					DeltaRhone1 - 2022					Both cruises		
Area	Station	TA Flux	DIC Flux	Taf:DICf	Station average	Domain average	TA Flux	DIC Flux	Taf:DICf	Station average	Domain average	TA fluxes Average area	DIC fluxes Average area	Taf:DICf ratio Average area
		mmol m² d⁻¹	mmol m² d⁻¹				mmol m² d⁻¹	mmol m² d⁻¹				mmol m² d⁻¹	mmol m² d⁻¹	
Proximal domain	Z	33.9	66.2	0.51	0.60	0.52	45.8	84.6	0.54	0.59	0.51	30 ± 21	54 ± 20	0.52
		20.5	46.3	0.44			-	53.4	-					
		78.5	92.0	0.85			24.3	42.0	0.58					
		-	-	-			27.0	42.2	0.64					
	A	15.6	45.6	0.34	0.41		8.7	33.2	0.26	0.46				
		16.2	49.1	0.33			26.1	58.2	0.45					
		30.7	55.8	0.55			11.3	23.9	0.47					
		-	-	-			21.5	32.9	0.65					
	AZ	16.5	47.3	0.35	0.55		-	-	-	-				
		20.7	49.6	0.42			-	-	-					
		78.7	90.4	0.87			-	-	-					
Prodeltaic domain	AK	-	35.2	-	0.25	0.26	7.0	37.9	0.18	0.25	0.25	6 ± 4	24 ± 11	0.26
		9.9	25.5	0.39			6.8	21.1	0.32					
		3.3	29.0	0.11			-	52.7	-					
		-	-	-			-	13.4	-					
	K	11.5	25.2	0.46	0.38		-	-		0.25				
		9.3	24.9	0.37			1.1	10.0	0.25					
		6.9	21.6	0.32			-	26.4	-					
		-	-				3.1	12.3	-					
	L	2.0	14.5	0.14	0.15				-	-				
		2.8	15.7	0.18					-					
		2.7	18.0	0.15					-					
Distal shelf	E	2.0	7.9	0.25	0.25	-0.16	-3.1	5.9	-0.52	-0.11	-0.11	-1 ± 2	8 ± 3	-0.14
		-	2.4	-				7.0	-					
		-	7.1	-			1.3	8.9	0.15					
		-	-	-			0.3	7.8	0.04					
	C	-2.9	13.5	-0.21	-0.30				-	-				
		-1.8	11.2	-0.16					-					
		-4.2	7.9	-0.53					-					

Figure B1 *: DIC and TA flux values and ratios for the MissRhoDia2 and DeltaRhone1 cruises for all cores at all investigated stations.*

https://doi.org/10.5194/egusphere-2026-5259
Preprint. Discussion started: 9 September 2026

Appendix C

		MissRhoDia2 - 2018				DeltaRhone1 - 2022				Both cruises	
Area	Station	TOU	DIC:TOU	Station average	Domain average	TOU	DIC:TOU	Station average	Domain average	TOU Average area	DIC/TOU Average area
		$mmol\ m^2\ d^{-1}$				$mmol\ m^2\ d^{-1}$					
Proximal domain	Z	23.8	2.78	2.52	2.39	24.4	3.47	1.80	2.02	27 ± 14	2.21
		27.8	1.67			74.0	0.72				
		29.7	3.10			29.0	1.45				
		-	-			27.2	1.55				
	A	21.8	2.09	2.27		9.9	3.36	2.24			
		23.5	2.09			33.2	1.75				
		21.1	2.64			13.2	1.82				
		-	-			16.3	2.02				
	AZ	19.2	2.47	2.39			-	-			
		29.5	1.68				-				
		29.8	3.03				-				
Prodelta	AK	23.8	1.48	1.23	1.37	9.2	4.13	1.82	1.46	18 ± 8	1.42
		28.6	0.89			17.1	1.23				
		22.0	1.32			39.9	1.32				
		-				22.1	0.61				
	K	13.5	1.86	1.51		12.1		0.98			
		17.9	1.39			17.4	0.57				
		17.1	1.27			21.4	1.23				
		-				10.8	1.14				
	L	13.9	1.04	1.37		-	-	-			
		9.7	1.62			-	-				
		12.5	1.44			-	-				
Distal shelf	E	9.0	0.88	0.69	0.84	-	-	1.35	1.35	9 ± 2	1.10
		8.1	0.30			4.4	1.58				
		8.0	0.89			5.7	1.58				
		-	-			8.6	0.91				
	C	11.6	1.17	1.00			-	-			
		10.0	1.12				-				
		11.0	0.72				-				

Figure C1 : *TOU values and DICflux: TOU ratios for the MissRhoDia2 and DeltaRhone1 cruises for all cores at all investigated stations.*

https://doi.org/10.5194/egusphere-2026-5259
Preprint. Discussion started: 9 September 2026

Code and Data Availability

All data used in this study are available through SEANOE (https://doi.org/10.17882/112245 , Ferreira et al.,2026.

Author contributions

Eva Ferreira : conceptualization, methodology, formal analysis, data curation, investigation, validation, visualization, writing – original draft preparation. Bruno Bombled : formal analysis, data curation, investigation. Bruno Lansard and Christophe Rabouille : supervision, funding acquisition, validation, investigation, methodology, writing-review and editing.

Competing interests

The authors declare that they have no conflicts of interest.

Disclaimer

Copernicus Publications remains neutral with regard to jurisdictional claims made in the text, published maps, institutional affiliations, or any other geographical representation in this paper. While Copernicus Publications makes every effort to include appropriate place names, the final responsibility lies with the authors. Views expressed in the text are those of the authors and do not necessarily reflect the views of the publisher.

Acknowledgments

We would like to thank the captains and crews of the RV Tethys II (CNRS and Ifremer) for their support and technical assistance during the operations at sea. We are grateful to Anouck Villedieu for incubator development and first deployment. We acknowledge Marine Manoux, Laurie Brethous and Antoine Rocipon for the help on benthic fluxes analysis on board and in the laboratory. DIC and TA measurements in the water column were conducted at SNAPO-CO2 in LOCEAN/IPSL (Paris, France). A previous version of this paper has benefited from valuable comments we would like to thank the anonymous reviewer.

Financial support

This work was funded by the INSU/EC2CO/LEFE project MissRhoDia (2017-2018), by the INSU/EC2CO programme DeltaRhône (2021-2023) and by the PPR-RiOMar project, a French government grant managed by the Agence Nationale de la Recherche under the France 2030 program, reference ANR 22 POCE 0006.

https://doi.org/10.5194/egusphere-2026-5259
Preprint. Discussion started: 9 September 2026

References

Ait Ballagh, F. E., Rabouille, C., Andrieux-Loyer, F., Soetaert, K., Lansard, B., Bombled, B., Monvoisin, G., Elkalay, K., and Khalil, K.: Spatial Variability of Organic Matter and Phosphorus Cycling in Rhône River Prodelta Sediments (NW Mediterranean Sea, France): a Model-Data Approach, Estuaries and Coasts, 44, 1765-1789, https://doi.org/10.1007/s12237-020-00889-9, 2021.

Aller, J. Y. and Stupakoff, I.: The distribution and seasonal characteristics of benthic communities on the Amazon shelf as indicators of physical processes, Continental Shelf Research, 16, 717-751, https://doi.org/10.1016/0278-4343(96)88778-4, 1996.

Anderson, L., G. , Hall, P., O. J. , Iverfeldt, A., Rutgers van der Loejf, M. M., Sundby, B., and Westerlund, S., F. G. : Benthic respiration measured by total carbonate production, Limnology and Oceanography, 31, 319-329, 10.4319/lo.1986.31.2.0319, 1986.

Andersson, A. J. and Mackenzie, F. T.: Revisiting four scientific debates in ocean acidification research, Biogeosciences, 9, 893-905, 10.5194/bg-9-893-2012, 2012.

Arndt, S., Jørgensen, B. B., LaRowe, D. E., Middelburg, J. J., Pancost, R. D., and Regnier, P.: Quantifying the degradation of organic matter in marine sediments: A review and synthesis, Earth-Science Reviews, 123, 53-86, http://dx.doi.org/10.1016/j.earscirev.2013.02.008, 2013.

Barbier, E. B., Hacker, S. D., Kennedy, C., Koch, E. W., Stier, A. C., and Silliman, B. R.: The value of estuarine and coastal ecosystem services, Ecological Monographs, 81, 169-193, https://doi.org/10.1890/10-1510.1, 2011.

Bauer, J. E., Cai, W.-J., Raymond, P. A., Bianchi, T. S., Hopkinson, C. S., and Regnier, P. A. G.: The changing carbon cycle of the coastal ocean, Nature, 504, 61-70, https://doi.org/10.1038/nature12857, 2013.

Burdige, D. J.: Preservation of organic matter in marine sediments: controls, mechanisms, and an imbalance in sediment organic carbon budgets?, Chemical Reviews, 107, 467-485, https://doi.org/10.1021/cr050347q, 2007.

Burdige, D. J. and Komada, T.: Anaerobic oxidation of methane and the stoichiometry of remineralization processes in continental margin sediments, Limnology and Oceanography, 56, 1781-1796, 2011.

Cai, W.-J., Hu, X., Huang, W.-J., Murrell, M. C., Lehrter, J. C., Lohrenz, S. E., Chou, W.-C., Zhai, W., Hollibaugh, J. T., Wang, Y., Zhao, P., Guo, X., Gundersen, K., Dai, M., and Gong, G.-C.: Acidification of subsurface coastal waters enhanced by eutrophication, Nature Geoscience, 4, 766-770, https://doi.org/10.1038/ngeo1297, 2011.

Canfield, D. E., Jørgensen, B. B., Fossing, H., Glud, R., Gundersen, J., Ramsing, N. B., Thamdrup, B., Hansen, J. W., Nielsen, L. P., and Hall, P. O. J.: Pathways of organic carbon oxidation in three continental margin sediments, Marine Geology, 113, 27-40, 1993.

Cathalot, C., Rabouille, C., Pastor, L., Deflandre, B., Viollier, E., Buscail, R., Grémare, A., Treignier, C., and Pruski, A.: Temporal variability of carbon recycling in coastal sediments influenced by rivers: assessing the impact of flood inputs in the Rhône River prodelta, Biogeosciences, 7, 1187-1205, https://doi.org/10.5194/bg-7-1187-2010, 2010.

Cathalot, C., Rabouille, C., Tisnérat-Laborde, N., Toussaint, F., Kerhervé, P., Buscail, R., Loftis, K., Sun, M. Y., Tronczynski, J., Azoury, S., Lansard, B., Treignier, C., Pastor, L., and Tesi, T.: The fate of river organic

https://doi.org/10.5194/egusphere-2026-5259
Preprint. Discussion started: 9 September 2026

carbon in coastal areas: A study in the Rhône River delta using multiple isotopic (δ13C, Δ14C) and organic tracers, Geochimica et Cosmochimica Acta, 118, 33-55, http://dx.doi.org/10.1016/j.gca.2013.05.001, 2013.

Charmasson, S., Bouisset, P., Radakovitch, O., Pruchon, A.-S., and Arnaud, M.: Long-core profiles of 137Cs, 134Cs, 60Co and 210Pb in sediment near the Rhone River (northwestern Mediterranean Sea), Estuaries, 21, 367-378, https://doi.org/10.2307/1352836, 1998.

Chen, C.-T. A. and Borges, A. V.: Reconciling opposing views on carbon cycling in the coastal ocean: Continental shelves as sinks and near-shore ecosystems as sources of atmospheric CO2, Deep Sea Research Part II: Topical Studies in Oceanography, 56, 578-590, https://doi.org/10.1016/j.dsr2.2009.01.001, 2009.

Chou, W.-C., Tishchenko, P. Y., Chuang, K.-Y., Gong, G.-C., Shkirnikova, E. M., and Tishchenko, P. P.: The contrasting behaviors of CO2 systems in river-dominated and ocean-dominated continental shelves: A case study in the East China Sea and the Peter the Great Bay of the Japan/East Sea in summer 2014, Marine Chemistry, 195, 50-60, https://doi.org/10.1016/j.marchem.2017.04.005, 2017.

Dai, M., Yin, Z., Meng, F., Liu, Q., and Cai, W.-J.: Spatial distribution of riverine DOC inputs to the ocean: an updated global synthesis, Current Opinion in Environmental Sustainability, 4, 170-178, https://doi.org/10.1016/j.cosust.2012.03.003, 2012.

Dai, M., Su, J., Zhao, Y., Hofmann, E. E., Cao, Z., Cai, W.-J., Gan, J., Lacroix, F., Laruelle, G. G., Meng, F., Müller, J. D., Regnier, P. A. G., Wang, G., and Wang, Z.: Carbon Fluxes in the Coastal Ocean: Synthesis, Boundary Processes, and Future Trends, Annual Review of Earth and Planetary Sciences, 50, 593-626, https://doi.org/10.1146/annurev-earth-032320-090746, 2022.

Denis, L. and Grenz, C.: Spatial variability in oxygen and nutrient fluxes at the sediment-water interface on the continental shelf in the Gulf of Lions (NW Mediterranean), Oceanologica Acta, 26, 373-389, https://doi.org/10.1016/S0399-1784(03)00017-3, 2003.

Dickson, A. G., Sabine, C. L., and Christian, J. R.: Guide to best practices for ocean CO2 measurement, Sidney, British Columbia, North Pacific Marine Science Organization. (PICES Special Publication 3; IOCCP Report 8), 191pp, 2007.

Dumoulin, J. P., Pozzato, L., Rassman, J., Toussaint, F., Fontugne, M., Tisnérat-Laborde, N., Beck, L., Caffy, I., Delqué-Količ, E., Moreau, C., and Rabouille, C.: Isotopic Signature (δ13C, Δ14C) of DIC in Sediment Pore Waters: An Example from the Rhone River Delta, Radiocarbon, 60, 1465-1481, 10.1017/RDC.2018.111, 2018.

Dumoulin, J. P., Copard, Y., Bombled, B., Pourtout, S., Beck, L., Delqué-Količ, E., Quiles, A., Caffy, I., Perron, M., Sieudat, M., Thellier, B., and Rabouille, C.: Tracing the origin of organic matter in river deltas using the dual isotopic composition of carbon (δ13C and Δ14C): A decade of study in sediments and porewaters of the Rhône River delta, Radiocarbon, 1-18, 10.1017/RDC.2026.10205, 2026.

Durrieu de Madron, X., Abassi, A., Heussner, S., Monaco, A., Aloisi, J. C., Radakovitch, O., Giresse, P., Buscail, R., and Kerherve, P.: Particulate matter and organic carbon budgets for the Gulf of Lions (NW Mediterranean), Oceanologica Acta, 23, 717-730, https://doi.org/10.1016/S0399-1784(00)00119-5, 2000.

Edmonds, D. A., Caldwell, R. L., Brondizio, E. S., and Siani, S. M. O.: Coastal flooding will disproportionately impact people on river deltas, Nature Communications, 11, 4741, 10.1038/s41467-020-18531-4, 2020.

https://doi.org/10.5194/egusphere-2026-5259
Preprint. Discussion started: 9 September 2026

Emerson, S. and Hedges, J.: Chemical Oceanography and the Marine Carbon Cycle, Cambridge University Press, Cambridge, https://doi.org/10.1017/CBO9780511793202, 2008.

Estournel, C., Kondrachoff, V., Marsaleix, P., and Vehil, R.: The plume of the Rhone: numerical simulation and remote sensing, Continental Shelf Research, 17, 899-924, https://doi.org/10.1016/S0278-4343(96)00064-7, 1997.

Estournel, C., Mikolajczak, G., Ulses, C., Bourrin, F., Canals, M., Charmasson, S., Doxaran, D., Duhaut, T., de Madron, X. D., Marsaleix, P., Palanques, A., Puig, P., Radakovitch, O., Sanchez-Vidal, A., and Verney, R.: Sediment dynamics in the Gulf of Lion (NW Mediterranean Sea) during two autumn–winter periods with contrasting meteorological conditions, Progress in Oceanography, 210, 102942, https://doi.org/10.1016/j.pocean.2022.102942, 2023.

Ferreira, E., Nmor, S., Viollier, E., Lansard, B., Bombled, B., Regnier, E., Monvoisin, G., Grenz, C., van Beek, P., and Rabouille, C.: Characterization of the benthic biogeochemical dynamics after flood events in the Rhône River prodelta: a data–model approach, Biogeosciences, 21, 711-729, 10.5194/bg-21-711-2024, 2024.

Ferreira, E.: Dynamique benthique des carbonates et acidification dans deux deltas contrastés : le cas du Rhône et du Mississippi., pH. D. thesis, LSCE, University Paris-Saclay, France, 253pp, https://theses.hal.science/tel-05501274, 2025.

Friedl, G., Dinkel, C., and Wehrli, B.: Benthic fluxes of nutrients in the northwestern Black Sea, Marine Chemistry, 62, 77-88, https://doi.org/10.1016/S0304-4203(98)00029-2, 1998.

Glud, R. N., Stahl, H., Berg, P., Wenzhöfer, F., Oguri, K., and Kitazato, H.: In situ Microscale Variation in Distribution and Consumption of O_2: A Case Study from a Deep Ocean Margin Sediment (Sagami Bay, Japan), Limnology and Oceanography, 54, 1-12, 2009.

Gordon, E. S. and Goñi, M. A.: Sources and distribution of terrigenous organic matter delivered by the Atchafalaya River to sediments in the northern Gulf of Mexico, Geochimica et Cosmochimica Acta, 67, 2359-2375, https://doi.org/10.1016/S0016-7037(02)01412-6, 2003.

Got, H. and Aloisi, J. C.: The Holocene sedimentation on the gulf of lions margin: a quantitative approach, Continental Shelf Research, 10, 841-855, https://doi.org/10.1016/0278-4343(90)90062-Q, 1990.

Hansen, H. P.: Determination of oxygen, in: Methods of Seawater Analysis, 75-89, https://doi.org/10.1002/9783527613984.ch4, 1999.

Hedges, J. I. and Keil, R. G.: Sedimentary organic matter preservation: an assessment and speculative synthesis, Marine Chemistry, 49, 81-115, https://doi.org/10.1016/0304-4203(95)00008-F, 1995.

Hedges, J. I., Keil, R. G., and Benner, R.: What happens to terrestrial organic matter in the ocean?, Organic Geochemistry, 27, 195-212, https://doi.org/10.1016/S0146-6380(97)00066-1, 1997.

Hu, X. and Cai, W.-J.: An assessment of ocean margin anaerobic processes on oceanic alkalinity budget, Global Biogeochemical Cycles, 25, https://doi.org/10.1029/2010GB003859, 2011.

Jørgensen, B. B., Wenzhöfer, F., Egger, M., and Glud, R. N.: Sediment oxygen consumption: Role in the global marine carbon cycle, Earth-Science Reviews, 228, 103987, https://doi.org/10.1016/j.earscirev.2022.103987, 2022.

Kononets, M., Tengberg, A., Nilsson, M., Ekeroth, N., Hylén, A., Robertson, E. K., van de Velde, S., Bonaglia, S., Rütting, T., Blomqvist, S., and Hall, P. O. J.: In situ incubations with the Gothenburg benthic chamber landers: Applications and quality control, Journal of Marine Systems, 214, 103475, https://doi.org/10.1016/j.jmarsys.2020.103475, 2021.

Krumins, V., Gehlen, M., Arndt, S., Van Cappellen, P., and Regnier, P.: Dissolved inorganic carbon and alkalinity fluxes from coastal marine sediments: model estimates for different shelf environments and sensitivity to global change, Biogeosciences, 10, 371-398, https://doi.org/10.5194/bg-10-371-2013, 2013.

Lansard, B., Rabouille, C., Denis, L., and Grenz, C.: Benthic remineralization at the land-ocean interface: A case study of the Rhône River (NW Mediterranean Sea), Estuarine, Coastal and Shelf Science, 81, 544-554, https://doi.org/10.1016/j.ecss.2008.11.025, 2009.

Ludwig, W., Dumont, E., Meybeck, M., and Heussner, S.: River discharges of water and nutrients to the Mediterranean and Black Sea: Major drivers for ecosystem changes during past and future decades?, Progress in Oceanography, 80, 199-217, https://doi.org/10.1016/j.pocean.2009.02.001, 2009.

Łukawska-Matuszewska, K. and Dwornik, M.: Early diagenesis in anoxic sediments of the Gulf of Gdańsk (southern Baltic Sea): Implications for porewater chemistry and benthic flux of carbonate alkalinity, Frontiers in Earth Science, Volume 13 - 2025, 10.3389/feart.2025.1593031, 2025.

Łukawska-Matuszewska, K. and Graca, B.: Pore water alkalinity below the permanent halocline in the Gdańsk Deep (Baltic Sea) - Concentration variability and benthic fluxes, Marine Chemistry, 204, 49-61, https://doi.org/10.1016/j.marchem.2018.05.011, 2018.

Magette, E., Boever, A., Bridgham, H., Ferreira, E., Silvera, O., Bombled, B., Beckler, J., Rabouille, C., and Taillefert, M.: Benthic biogeochemical reactions and fluxes in the hypoxic and acidified northern Gulf of Mexico (nGoM), part III: Seasonal and spatial variability of in-situ benthic alkalinity and dissolved inorganic carbon fluxes, Marine Chemistry, submitted.

Maillet, G. M., Vella, C., Berne, S., Friend, P. L., Amos, C. L., Fleury, T. J., and Normand, A.: Morphological changes and sedimentary processes induced by the December 2003 flood event at the present mouth of the Grand Rhone River (southern France), Marine Geology, 234, 159-177, https://doi.org/10.1016/j.margeo.2006.09.025, 2006.

McKee, B. A., Aller, R. C., Allison, M. A., Bianchi, T. S., and Kineke, G. C.: Transport and transformation of dissolved and particulate materials on continental margins influenced by major rivers: benthic boundary layer and seabed processes, Continental Shelf Research, 24, 899-926, https://doi.org/10.1016/j.csr.2004.02.009, 2004.

Metzl, N., Fin, J., Lo Monaco, C., Mignon, C., Alliouane, S., Bombled, B., Boutin, J., Bozec, Y., Comeau, S., Conan, P., Coppola, L., Cuet, P., Ferreira, E., Gattuso, J. P., Gazeau, F., Goyet, C., Grossteffan, E., Lansard, B., Lefèvre, D., Lefèvre, N., Leseurre, C., Petton, S., Pujo-Pay, M., Rabouille, C., Reverdin, G., Ridame, C., Rimmelin-Maury, P., Ternon, J. F., Touratier, F., Tribollet, A., Wagener, T., and Wimart-Rousseau, C.: An updated synthesis of ocean total alkalinity and dissolved inorganic carbon measurements from 1993 to 2023: the SNAPO-CO2-v2 dataset, Earth Syst. Sci. Data, 17, 1075-1100, https://doi.org/10.5194/essd-17-1075-2025, 2025.

Miralles, J., Radakovitch, O., and Aloïsi, J. C.: 210Pb sedimentation rates from the Northwestern Mediterranean margin, Marine Geology, 216, 155-167, https://doi.org/10.1016/j.margeo.2005.02.020, 2005.

Nmor, S. I., Viollier, E., Pastor, L., Lansard, B., Rabouille, C., and Soetaert, K.: FESDIA (v1.0): exploring temporal variations of sediment biogeochemistry under the influence of flood events using numerical modelling, Geosci. Model Dev., 15, 7325-7351, https://doi.org/10.5194/gmd-15-7325-2022, 2022.

Pastor, L., Deflandre, B., Viollier, E., Cathalot, C., Metzger, E., Rabouille, C., Escoubeyrou, K., Lloret, E., Pruski, A. M., Vétion, G., Desmalades, M., Buscail, R., and Grémare, A.: Influence of the organic matter composition on benthic oxygen demand in the Rhône River prodelta (NW Mediterranean Sea), Continental Shelf Research, 31, 1008-1019, https://doi.org/10.1016/j.csr.2011.03.007, 2011.

Pierrot, D., Lewis, E., and Wallace, D. W. R.: MS Excel Program Developed for CO2 System Calculations. , ORNL/CDIAC-105a. Carbon Dioxide Information Analysis Center, Oak Ridge National Laboratory, U.S. Department of Energy, Oak Ridge, Tennessee., doi: 10.3334/CDIAC/otg.CO2SYS_XLS_CDIAC105a, 2006.

Pont, D., Simonnet, J.-P., and Walter, A. V.: Medium-term changes in suspended sediment delivery to the ocean: consequences of catchment heterogeneity and river management (Rhône River, France), Estuarine, Coastal and Shelf Science, 54, 1-18, 2002.

Pozzato, L., Rassmann, J., Lansard, B., Dumoulin, J.-P., van Breugel, P., and Rabouille, C.: Origin of remineralized organic matter in sediments from the Rhone River prodelta (NW Mediterranean) traced by Δ14C and δ13C signatures of pore water DIC, Progress in Oceanography, 163, 112-122, https://doi.org/10.1016/j.pocean.2017.05.008, 2018.

Rabouille, C., Conley, D. J., Dai, M. H., Cai, W. J., Chen, C. T. A., Lansard, B., Green, R., Yin, K., Harrison, P. J., Dagg, M., and McKee, B.: Comparison of hypoxia among four river-dominated ocean margins: The Changjiang (Yangtze), Mississippi, Pearl, and Rhône rivers, Continental Shelf Research, 28, 1527-1537, https://doi.org/10.1016/j.csr.2008.01.020, 2008.

Rassmann, J., Lansard, B., Pozzato, L., and Rabouille, C.: Carbonate chemistry in sediment porewaters of the Rhône River delta driven by early diagenesis (northwestern Mediterranean), Biogeosciences, 13, 5379-5394, https://doi.org/10.5194/bg-13-5379-2016, 2016.

Rassmann, J., Eitel, E. M., Lansard, B., Cathalot, C., Brandily, C., Taillefert, M., and Rabouille, C.: Benthic alkalinity and dissolved inorganic carbon fluxes in the Rhône River prodelta generated by decoupled aerobic and anaerobic processes, Biogeosciences, 17, 13-33, https://doi.org/10.5194/bg-17-13-2020, 2020.

Regnier, P., Friedlingstein, P., Ciais, P., Mackenzie, F. T., Gruber, N., Janssens, I. A., Laruelle, G. G., Lauerwald, R., Luyssaert, S., Andersson, A. J., Arndt, S., Arnosti, C., Borges, A. V., Dale, A. W., Gallego-Sala, A., Goddéris, Y., Goossens, N., Hartmann, J., Heinze, C., Ilyina, T., Joos, F., LaRowe, D. E., Leifeld, J., Meysman, F. J. R., Munhoven, G., Raymond, P. A., Spahni, R., Suntharalingam, P., and Thullner, M.: Anthropogenic perturbation of the carbon fluxes from land to ocean, Nature Geoscience, 6, 597-607, 10.1038/ngeo1830, 2013.

Regnier, P., Resplandy, L., Najjar, R. G., and Ciais, P.: The land-to-ocean loops of the global carbon cycle, Nature, 603, 401-410, https://doi.org/10.1038/s41586-021-04339-9, 2022.

Rowe, G. T., Kaegi, M. E. C., Morse, J. W., Boland, G. S., and Escobar Briones, E. G.: Sediment community metabolism associated with continental shelf hypoxia, Northern Gulf of Mexico, Estuaries, 25, 1097-1106, https://doi.org/10.1007/BF02692207, 2002.

Sempéré, R., Charrière, B., Van Wambeke, F., and Cauwet, G.: Carbon inputs of the Rhône River to the Mediterranean Sea: Biogeochemical implications, Global Biogeochemical Cycles, 14, 669-681,

https://doi.org/10.5194/egusphere-2026-5259
Preprint. Discussion started: 9 September 2026

https://doi.org/10.1029/1999gb900069, 2000.

Tengberg, A., Hovdenes, J., Andersson, H. J., Brocandel, O., Diaz, R., Hebert, D., Arnerich, T., Huber, C., Körtzinger, A., Khripounoff, A., Rey, F., Rönning, C., Schimanski, J., Sommer, S., and Stangelmayer, A.: Evaluation of a lifetime-based optode to measure oxygen in aquatic systems, Limnology and Oceanography: Methods, 4, 7-17, https://doi.org/10.4319/lom.2006.4.7, 2006.

Thill, A., Moustier, S., Garnier, J.-M., Estournel, C., Naudin, J.-J., and Bottero, J.-Y.: Evolution of particle size and concentration in the Rhône river mixing zone:: influence of salt flocculation, Continental Shelf Research, 21, 2127-2140, https://doi.org/10.1016/S0278-4343(01)00047-4, 2001.

Thomas, H., Schiettecatte, L. S., Suykens, K., Koné, Y. J. M., Shadwick, E. H., Prowe, A. E. F., Bozec, Y., de Baar, H. J. W., and Borges, A. V.: Enhanced ocean carbon storage from anaerobic alkalinity generation in coastal sediments, Biogeosciences, 6, 267-274, https://doi.org/10.5194/bg-6-267-2009, 2009.

van Dam, B., Lehmann, N., Zeller, M. A., Neumann, A., Pröfrock, D., Lipka, M., Thomas, H., and Böttcher, M. E.: Benthic alkalinity fluxes from coastal sediments of the Baltic and North seas: comparing approaches and identifying knowledge gaps, Biogeosciences, 19, 3775-3789, 10.5194/bg-19-3775-2022, 2022.

van de Velde, S. J., Hylén, A., and Meysman, F. J. R.: Ocean alkalinity destruction by anthropogenic seafloor disturbances generates a hidden CO₂ emission, Science Advances, 11, eadp9112, doi:10.1126/sciadv.adp9112, 2025.

van Loenen, O., S., , Bombled, B., Regnier, E., Rigaud, S., Viollier, E., Lansard, B., Ferreira, E., Radakovitch, O., Dumoulin, J.-P., Pairaud, I., Bourrin, F., and Rabouille, C.: Impact of floods and primary production on benthic DO, DIC and AT fluxes: year-round time-series in the Rhône River prodelta, Available at SSRN: http://dx.doi.org/10.2139/ssrn.6726403 2026. 6 May 2026., preprint

Wolf-Gladrow, D. A., Zeebe, R. E., Klaas, C., Körtzinger, A., and Dickson, A. G.: Total alkalinity: The explicit conservative expression and its application to biogeochemical processes, Marine Chemistry, 106, 287-300, https://doi.org/10.1016/j.marchem.2007.01.006., 2007.

Yin, D., Cui, L., Harris, C. K., Moriarty, J. M., Beck, H., and Maiti, K.: The Role of Benthic Fluxes in Acidifying the Bottom Waters in the Northern Gulf of Mexico Hypoxic Zone Based on an Updated Water Column Biogeochemical-Seabed Diagenetic and Sediment Transport Model, Journal of Advances in Modeling Earth Systems, 16, e2023MS004045, https://doi.org/10.1029/2023MS004045, 2024.

Zhang, W., Xu, K., Herke, C., Alawneh, O., Jafari, N., Maiti, K., Clower, P. O., Glaspie, C. N., Tupitza, J. C., and Xue, Z. G.: Spatial and temporal variations of seabed sediment characteristics in the inner Louisiana shelf, Marine Geology, 463, 107115, https://doi.org/10.1016/j.margeo.2023.107115, 2023.